Polar Record 48 (244): 83–93 (2012). © *Her Majesty the Queen in right of Canada 2011.*
Published by Cambridge University Press. doi:10.1017/S0032247411000477

A method for trend-based change analysis in Arctic tundra using the 25-year Landsat archive

Robert Fraser, Ian Olthof, Mélanie Carrière, Alice Deschamps, and Darren Pouliot

Natural Resources Canada, Earth Sciences Sector, Canada Centre for Remote Sensing, 588 Booth St., Ottawa, ON, K1A0Y7, Canada (Robert.Fraser@NRCan.gc.ca)

ABSTRACT. Remote sensing has provided evidence of vegetation changes in Arctic tundra that may be attributable to recent climate warming. These changes are evident from local scales as expanding shrub cover observed in aerial photos, to continental scales as greening trends based on satellite vegetation indices. One challenge in applying conventional two date, satellite change detection in tundra environments is the short growing season observation window, combined with high inter-annual variability in vegetation conditions. We present an alternative approach for investigating tundra vegetation and surface cover changes based on trend analysis of long-term (1985-present) Landsat TM/ETM+ image stacks. The Tasseled Cap brightness, greenness, and wetness indices, representing linear transformations of the optical channels, are analysed for per-pixel trends using robust linear regression. The index trends are then related to changes in fractional shrub and other vegetation covers using a regression tree classifier trained with high resolution land cover. Fractional trends can be summarised by vegetation or ecosystem type to reveal any consistent patterns. Example results are shown for a 3 000 km^2 study area in northern Yukon, Canada where index and fractional changes are related to growth of vascular plants and coastal erosion.

Introduction

There is mounting evidence of vegetation and other physical changes in the Arctic and sub-Arctic associated with recent climate warming. Analysis of satellite based vegetation indices has revealed a greening trend over many northern regions thought to be caused by an increase in vegetation growth and longer growing seasons (Goetz and others 2005; Jia and others 2009; Pouliot and others 2009; Bhatt and others 2010). At local scales, comparison of historical and current air photos has documented a widespread increase in shrub growth over Alaska (Sturm and others 2001; Tape and others 2006) and northern Quebec (B. Tremblay, personal communication, 2010). Repeat plot measurements are also beginning to show decadal increases in vegetation productivity in Alaska (Gould and others 2009) and Canada's high Arctic (Hudson and Henry 2009; Hill and Henry 2010). Other recent Arctic changes that have been observed using remote sensing include coastline erosion (Mars and Houseknecht 2007; Lantuit and Pollard 2008), glacier retreat (Dowdeswell and others 2007), and a reduction in the area of lakes and shallow ponds (Riordan and others 2006; Labrecque and others 2009).

The majority of satellite remote sensing studies investigating changes to northern vegetation have been conducted using archived, coarse resolution (1–8 km) NOAA-AVHRR imagery, as summarised in Pouliot and others (2009). Although these data have the advantage of providing frequent continental scale coverage, their large heterogeneous pixels permit only regional analysis of productivity trends. Landsat imagery provides a means of analysing Arctic change over a similar 25 year time span, but at a 30 m resolution that is capable of resolving landscape scale changes and identifying particular vegetation types being impacted (Silapaswan and others 2001; Olthof and others 2008). The cost limitation for Landsat imagery was removed in 2008 with the opening of the USGS Landsat archive, providing a source of 30 m imagery from 1984 to present that can be used for land surface change studies. Landsat-5 and -7 continue to provide imagery in 2010, while the Landsat Data Continuity Mission scheduled for launch in 2012 will ensure a future source of no-cost data.

Many climate driven changes to Arctic vegetation are expected to be gradual and subtle in comparison to disturbances addressed in remote sensing studies of forested environments (Cohen and Others 2002; Fraser and others 2009). Changes in Arctic vegetation may include growth of vegetation to denser, higher biomass classes, such as low shrub to tall shrub (Stow and others 2004), expansion of shrub cover (Tape and others 2006), or shifts in vegetation community composition, such as moss and lichen being overtaken by shrub (Walker and others 2006). Fortunately, the foliar shrub component of tundra vegetation, the major change target of interest, exerts a strong influence on spectral reflectance (Stow and others 1993; Riedel and others 2005).

Change detection in the Arctic is complicated by variation in the satellite signal produced by factors unrelated to directional vegetation change. These include illumination effects and shadowing arising from steep solar angles and a frequently mountainous terrain, a short growing season with rapidly changing vegetation phenology, and atmospheric effects including haze and persistent cloud cover (Stow and others 2004). Large inter-annual differences in tundra vegetation growth (Epstein and others 2004; Boelman and others 2005; Buus-Hinkler and others 2006) due to climate variability could also render conventional two-date change detection results unrepresentative of longer term trends.

These challenges for measuring Arctic vegetation change using medium resolution imagery could be partially addressed by employing more frequent satellite observations. A recent development for Landsat based change detection is the use of dense temporal stacks of imagery rather than image pairs for monitoring forest and rangeland dynamics (Kennedy and others 2007; Goodwin and others 2008; Röder and others 2008; Huang and others 2010; Vogelmann and others 2009; Kennedy and others 2010). This approach is based on analysing the temporal trajectory of pixel level spectral values and may involve identifying temporal signatures characteristic of specific change events, segmenting the spectral trajectory, or linear trend analysis (Kennedy and others 2007; Goodwin and others 2008; Röder and others 2008; Kennedy and others 2010). The use of image stacks for northern change detection should allow real trend signals to be more reliably discerned from the sources of inter-scene and inter-annual variability described above.

A second strategy that could increase the ability to detect subtle, Arctic vegetation changes is to map land cover as a continuous rather than categorical variable. Olthof and Fraser (2007) compared three different methods (least squares inversion, linear regression, and regression trees) to map per-pixel land cover fractions from Landsat imagery over three northern locations in Canada. They found that regression tree modeling was the best overall method, producing an average bias of less than 3%. In another study (Selkowitz 2010), fractional land cover classification of Landsat imagery based on regression trees was found to be effective for mapping regional baseline levels of shrub canopy cover in northern Alaska. By contrast, a 'hard' classification change approach that assigns single land cover labels will be sensitive only to strong surface changes occurring over an entire pixel.

In this paper, we present a method for Landsat based change analysis in tundra environments that exploits the image stack and fractional mapping approaches described above. Coarse resolution NOAA-AVHRR data are also used to ensure that scenes selected for the image stack are representative of peak growing season conditions (Olthof and others 2008). The method is demonstrated in a coastal area of northern Yukon Territory, Canada.

Methods

Study area

Fig. 1 shows the approximately 3000 km^2 study area in northern Yukon used to demonstrate the stack based change method. The area includes a portion of Ivvavik National Park and Herschel Island, lying about 5 km north of the Beaufort Sea coastline. Major ecosystem types include cottongrass tussock tundra and polygonal wetlands on the gently sloping coastal plain, birch-willow low shrub communities on the mountain foothills to the south, and tall shrub riparian communities throughout (Parks Canada Agency 2009).

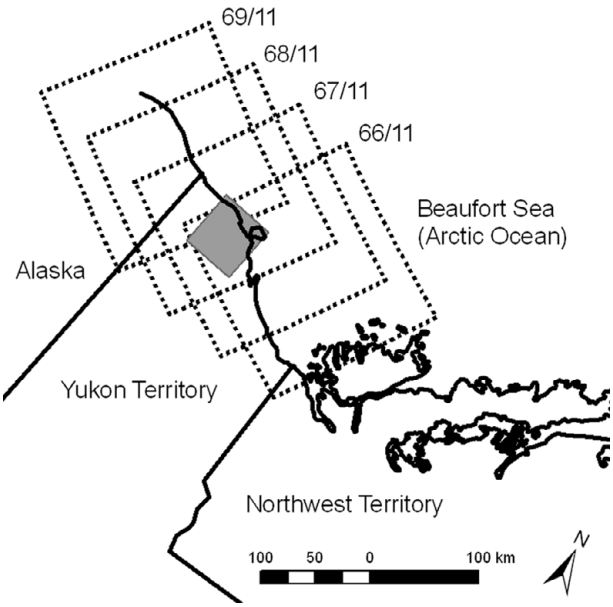

Fig. 1. Location of study area in northern Yukon Territory, Canada. The dashed lines indicate the footprint of the four WRS-2 Landsat frames used for the change analysis.

Building a Landsat image stack

Fig. 2 shows the major steps used to map fractional change in vegetation and land cover. The first step involves constructing a multi-year Landsat image stack. First, optimal path-row frames from the Worldwide Reference System-2 (WRS-2) covering the area of interest are selected. Since the method benefits from frequent observations, we exploited the more than 50% overlap of WRS-2 paths in the north and selected four adjacent frames (Fig. 1). A search of the USGS GloVis online catalogue revealed 23 Landsat scenes since 1984, providing at least partial clear sky coverage for the nominal 1 July–31 August growing season period. These were supplemented using three scenes purchased from the Canadian CEOCat3 archive, for a total of 26 candidate scenes (Table 1). Note that the GloVis level one terrain corrected (L1T) product has sub-pixel multi-temporal registration accuracy, which is essential for any pixel level change analysis.

A potential pitfall in analysing multi-year Landsat scenes for northern trend detection is that acquisition dates may often not coincide with peak vegetation phenology, which typically occurs in late July to early August. If the selection of scenes is not random about this peak (for example later years tend to be closer to or further away from the peak), this could create a bias and artificial trend in the time series. To avoid using scenes that deviate strongly from peak growing conditions, we characterised annual phenology cycles using 1-km NDVI values from NOAA-AVHRR 10 day composite data available for 1985–2008 (Latifovic and others 2005). To track phenology only over vegetated areas, green targets were selected that lie plus one standard deviation from the multi-year average of maximum annual NDVI

https://doi.org/10.1017/S0032247411000477 Published online by Cambridge University Press

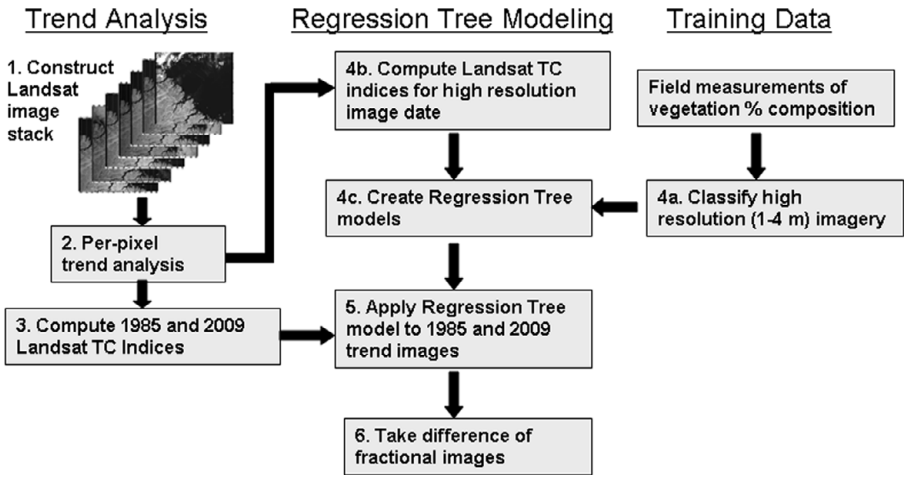

Fig. 2. Major steps required to perform trend and land cover fraction change analysis using Landsat image stacks.

over the entire study area. By calculating the average 10 day NDVI phenology profile over these vegetated pixels, the NDVI value corresponding to each Landsat acquisition date could be compared to peak NDVI for that year. This technique can then be used to pre-screen candidate Landsat scenes or to ensure that a final set of scenes does not exhibit any temporal trend in deviation from peak-phenology. After a further visual quality assessment and phenology screening of the candidate scenes, 16 of the 26 were selected for trend analysis (Table 1). When scene NDVI deviation from peak NDVI was regressed against year for these scenes, no significant ($p < 0.05$) trend was observed, suggesting no sampling bias.

Before building and analysing the image stack, pre-processing steps were applied to each Landsat scene as follows.

1. Radiometric calibration using coefficients that anchor the definitive calibration record for Landsat-5 TM to the Landsat-7 ETM radiometric scale (Chander and others 2009).
2. Calculation of top-of-atmosphere (TOA) reflectance.

Although theoretically desirable, accurate atmospheric correction to surface reflectance is challenging for early Landsat scenes, since historical atmospheric data are coarse. One potential option is to correct a recent Landsat scene, then radiometrically normalise other scenes to it based on stable, no change areas (Fraser and others 2009; Kennedy and others 2010). However, we opted not to normalise for this application because this could attenuate the signal from real changes if they were occurring over extensive

Table 1. Landsat scenes selected and pre-processed by WRS path/row. The final set of 16 scenes used for trend analysis is shown in italics.

Path/Row	**67/11**	**68/11**	**69/11**	**66/11**
Date 1	*12.8.2009 L5*			21.8.2009 L5
Date 2		24.8.2008 L7		
Date 3	*23.8.2007 L5*	30.8.2007 L5		
Date 4		*22.8.2007 L7*		
Date 5		5.7.2007 L7		
Date 6		*26.7.2006 L5*		
Date 7	*24.7.2005 L7*			
Date 8		21.8.2004 L5		
Date 9	16.7.2002 L7			
Date 10	30.8.2001 L7	*21.8.2001 L7*		
Date 11		*2.8.2000 L7*		
Date 12			*14.7.1999 L5*	
Date 13		*20.7.1998 L5*		
Date 14		12.7.1995 L5		
Date 15		*10.8.1994 L5*		*27.7.1994 L5*
Date 16	*15.7.1993 L5*			
Date 17	*28.7.1992 L5*	20.8.1992 L5		*6.8.1992 L5*
Date 19	12.7.1986 L5	*4.8.1986 L5*		
Date 20		*1.8.1985 L5*		

https://doi.org/10.1017/S0032247411000477 Published online by Cambridge University Press

areas of a scene (for example from widespread shrub growth).

3. Masking of cloud, cloud shadow, and data gaps in post-2003 SLC-off ETM+ scenes. Clouds and shadow were digitised against a clear sky reference image for this study. Automated cloud and shadow masking using thresholds may also be performed (Irish and others 2006), but in our experience can be inaccurate over bright northern land surfaces and areas subject to topographic shadowing. SLC-off gaps were treated as missing observations, similar to cloud.
4. Computing the Tasseled Cap (TC) indices (Crist and Cicone 1984; Huang and others 2002). These are linear transformations of the six Landsat optical bands into brightness, greenness, and wetness indices that typically capture 95% or more of their information content. The TC indices also have the advantage of being interpretable in terms of physical characteristics of the land surface. The Normalised Difference Vegetation Index (NDVI), which is highly correlated to TC greenness, was also calculated as a standard index.

Pixel-level trend analysis

The primary goal of this method is to map gradual, long term changes to vegetation. This is accomplished using a robust linear regression technique called Theil-Sen (Kendall and Stuart 1967) applied to each pixel time series in the image stack. Theil-Sen is a rank based regression technique in which slope is calculated from the median of all possible pair-wise slopes. It is resistant to up to 29% outliers, which in this case could represent pixels impacted by atmosphere, snow, or antecedent rainfall, or scenes that deviate from peak phenology that were not screened. The significance (p-value) of the rank based correlation coefficient tau, which is a measure of the strength of the monotonic relationship between x and y, is computed for each pixel. Synthetic TC images were also generated for the first and last stack date using each pixel's regression slope and offset (step 3), and were later used to estimate fractional land cover changes.

Regression tree modeling

Regression tree modeling provides an effective means of estimating the fractional land cover composition of pixels (Xu and others 2005; Olthof and Fraser 2007; Selkowitz 2010). Regression trees are used here to model sub-pixel Landsat fractions by relating fractional pixel land cover composition derived from a high resolution classification to Landsat TC index values. The model can then be applied to the first and last image stack date to derive long-term fractional land cover change.

A land cover classification based on high resolution (1–4 m) imagery is used to quantify 30 m land cover fractions within the corresponding Landsat subset window (step 4a). For the study area, an Ikonos scene from 4 August 2004 was co-registered to a clear sky

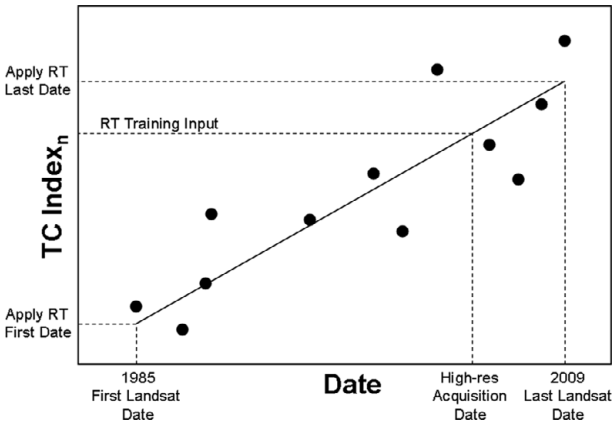

Fig. 3. Approach used to extract tasseled cap index values for training and applying the regression tree models based on a regression trend computed for each pixel's unique database.

Landsat scene from 24 July 2005 using image correlation (RMS = 1.0 m using 42 tie points) (step 4b). Four basic land cover classes (shrub, bare, herbaceous, and water) were assigned to the Ikonos scene based on their dominance within the 4 m pixels by labelling 60 spectral clusters resulting from fuzzy k-means unsupervised classification. Clusters were labelled using aerial photos acquired during summer 2008 that were georeferenced and mosaiced. The fractional composition of each 30 m Landsat pixel within the 80 km^2 Ikonos scene was then determined by summing the 4 m land cover classes within the spatially coincident 8–by–8 pixel (32–by–32 m) footprint.

The Cubist regression tree package by Rulequest Research was used to construct trees to predict the 30 m fractions for each class based on the three TC regression trend values corresponding to the Ikonos date (step 4c). Trees could then be applied to the TC regression trend values derived for 1985 and 2009 (Fig. 3). In cases where pixels did not display significant ($p < 0.05$) trends in a given TC index, the mean TC value from all pixel-level observations in the Landsat stack was used and held constant. A simple differencing of fractions from 1985 and 2009 quantified the changes predicted during the Landsat observation period.

Another option for training the regression trees would be to use actual TC values from the Landsat scene lying closest to the IKONOS image date instead of trend-based values. This option was evaluated by training trees using a Landsat scene from 24 July 2005, then applying it to a consecutive, near-anniversary date (26 July 2006) to evaluate the consistency of results.

Results

Fig. 4 shows the number of clear sky observations in each pixel's data stack after masking cloud, shadow, and SLC-off gaps in the 16 input scenes. The resulting minimum number of observations was 5 and the maximum 15. On average, 10.4 clear sky observations were available for

https://doi.org/10.1017/S0032247411000477 Published online by Cambridge University Press

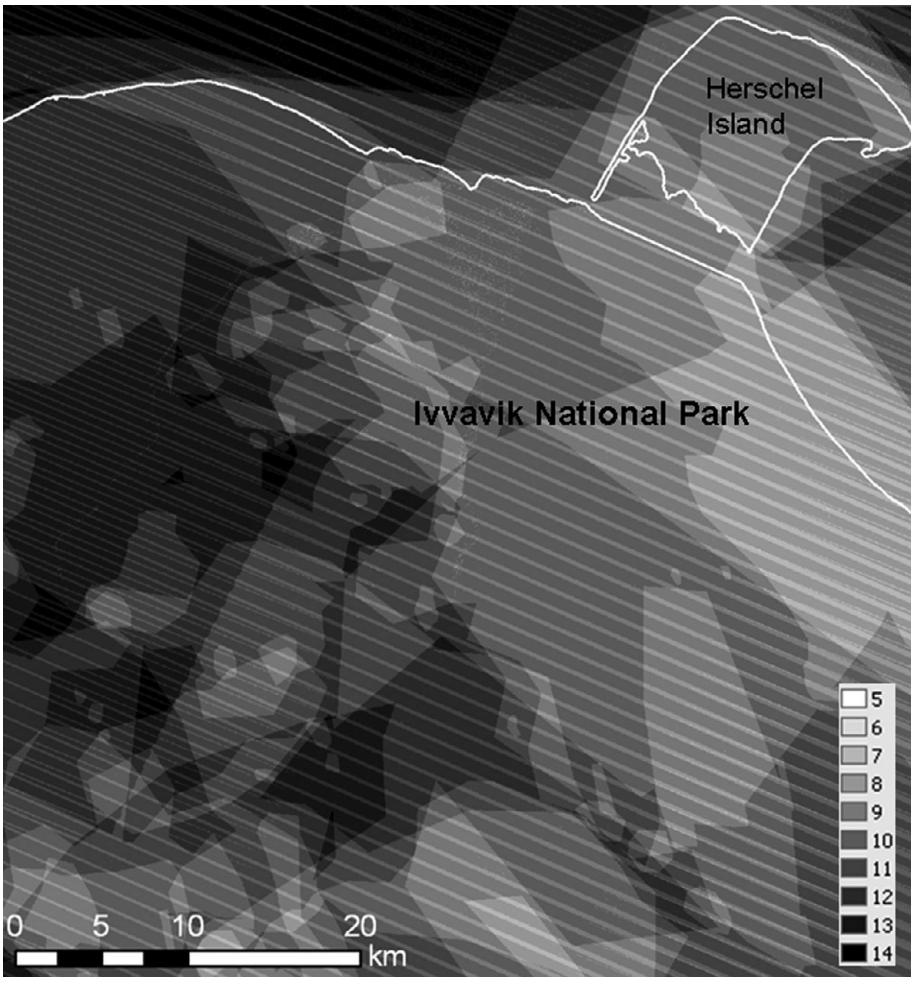

Fig. 4. Number of clear-sky, growing season Landsat observations over the study area for the period 1985–2009.

each pixel, which is equivalent to one observation every 2.5 years.

Fig. 5 displays the significant ($p < 0.05$) pixel-level TC brightness, greenness, and wetness index regression trends. Table 2 shows the percentage of the study area (omitting ocean) in which each index did not change, decreased, or increased. The near-infrared channel from the 2004 scene is provided for visual reference. The prominent trends observed were a widespread decreasing brightness, an increasing greenness, especially near the coast and on Herschel Island, and a variable change in wetness with most decreases occurring on steep south-westerly aspects and in areas of dynamic river braiding on the coastal plain.

The regression tree models used to determine baseline 30 m land cover fractions were evaluated using a random 30% holdout sample (Table 3). Comparing the estimated and calculated 30 m fractions, average absolute errors ranged from 5.1–12.4% and linear coefficients of determination (R^2) ranged from 0.48–0.86. Overall, these model results are comparable to those obtained by Olthof and Fraser (2007) for mapping Landsat fractions in other areas of northern Canada. The regression trees were also evaluated at 90 m resolution by aggregating fractions within 3–by–3 blocks of 30 m pixels to minimise the impact of misregistration error between the Landsat and Ikonos images. This had the effect of decreasing average prediction error to the range 3.7–8.6% and increasing R^2 values to 0.61–0.92. Selkowitz (2010) used a similar regression tree approach to map fractional shrub canopy (>0.5 m tall) on the coastal plain of Alaska. An aggregated 60 m validation resolution produced R^2 values of 0.44 or 0.59 and RMSE of 7.1 or 5.6 percent using two different training Landsat scenes. By comparison, we obtained an R^2 of 0.61 and 5.3% error for shrub evaluated at 90 m resolution.

Table 2 shows the proportion of the study area over which each basic land cover class stayed constant, decreased, and increased between 1985 and 2009. Average change for each class is also shown. Fig. 6 displays those areas that are predicted to be increasing and decreasing in each land cover class between 1985 and 2009. Note that many areas on Herschel Island and the coastal plain demonstrating an increase in TC greenness (Fig. 5) were also observed to have increasing shrub and herbaceous fractions, and a decreasing bare fraction (Fig. 6). Several

https://doi.org/10.1017/S0032247411000477 Published online by Cambridge University Press

Table 2. Percentage of the study area (omitting ocean) where each Tasseled Cap index and land cover fraction did not change, decreased, or increased. Average change for each index and class is also shown.

	TCB	TCG	TCW	Bare	Herb	Shrub	Water
% Area no change	82.0	91.6	90.3	66.3	70.1	71.7	75.7
% Area decreasing	17.4	0.8	6.5	28.0	14.7	4.7	7.8
% Area increasing	0.6	7.6	3.1	5.6	15.2	23.6	16.6
Average change (%)				−7.7	0.2	5.7	1.8

Table 3. Evaluation of regression tree models for bare, herbaceous, shrub, and water land cover fractions at 30 m and 90 m resolution using a random 30% holdout sample. All coefficients are highly significant ($p < 0.001$).

	Bare	Herb	Shrub	Water
Average absolute % error (30m)	12.4	6	7.6	5.1
Average absolute % error (90m)	8.6	3.8	5.3	3.7
R^2 Coefficient (30m)	0.64	0.61	0.48	0.86
R^2 Coefficient (90m)	0.75	0.78	0.61	0.92

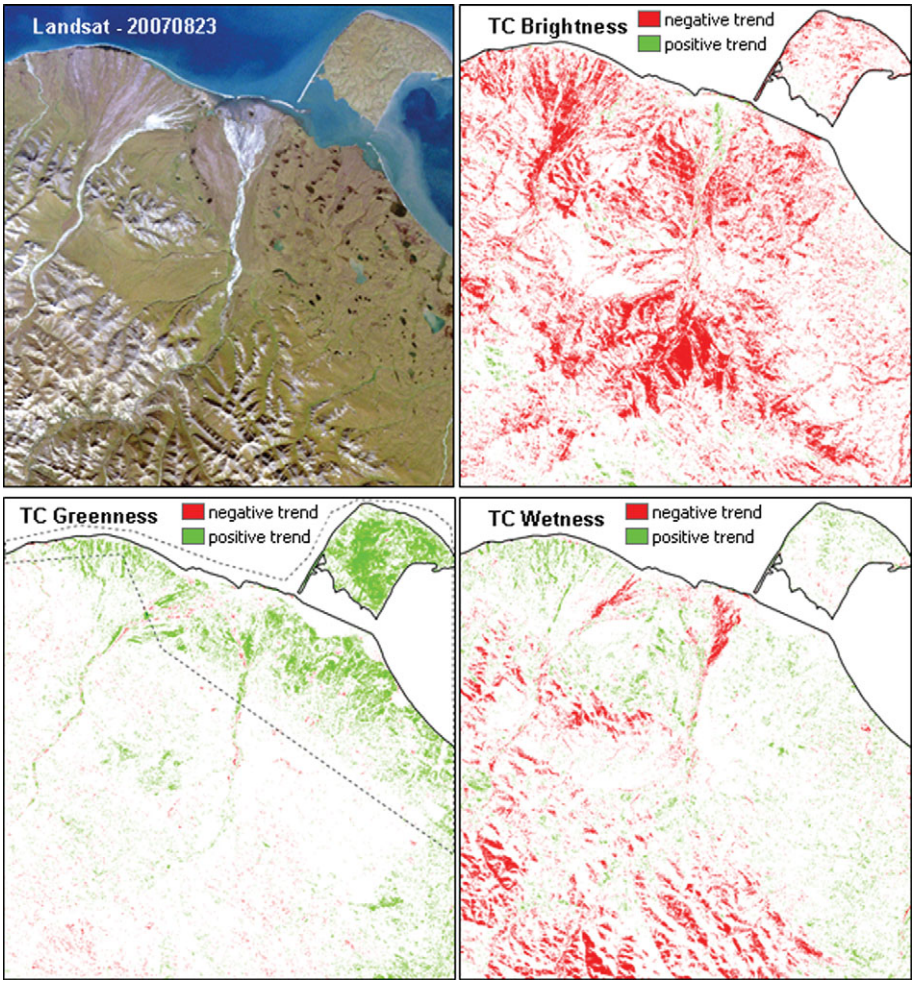

Fig. 5. 1985–2009 trends in the tasseled cap brightness, greenness, and wetness indices over the study area. The Landsat image is provided for visual reference. The dashed line in the greenness panel represents the portion of the study area where repeat field observations are available.

https://doi.org/10.1017/S0032247411000477 Published online by Cambridge University Press

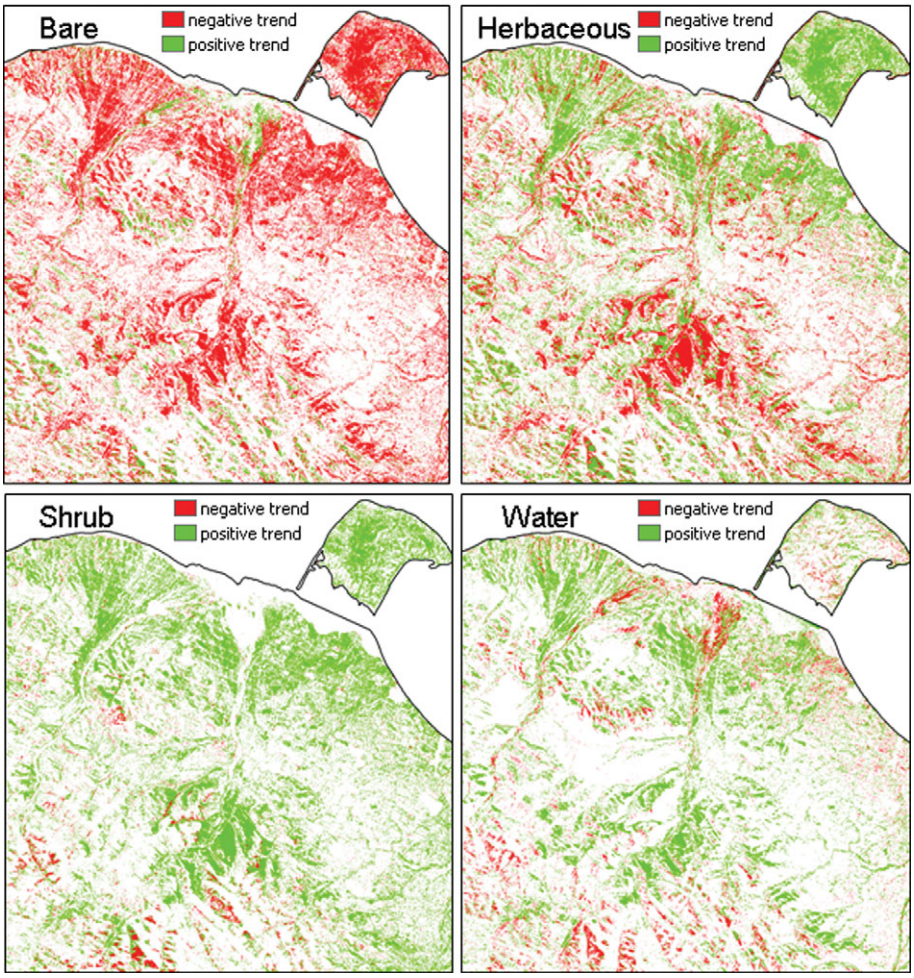

Fig. 6. 1985–2009 change in fractional land cover over the study area modeled using regression tree models.

large patches in the mountain foothills (centre of study area) showed a unique pattern of shrub increase with a corresponding decrease in the herbaceous and/or bare fraction. This vegetation consists of graminoid tussock mixed with varying amounts of willow and birch, and exposed rocky soil at higher elevations. Note that these patches were associated with a drop in TC brightness but surprisingly little or no change in greenness. This could be attributable to the lower visible reflectance of shrub compared to graminoid and bare ground (Stow and others 1993). The net result of these spatial trends was a predicted average decrease in bare of 7.7%, balanced by an increase in shrub of 5.7% over the study area.

The predicted fractional changes can also be summarised by land cover or ecosystem type the better to understand which vegetation types are exhibiting the largest changes. For this, a land cover classification product for northern Canada was used based on circa 2000 Landsat imagery (Olthof and others 2009). The average fractional change within each land cover class is summarised in Fig. 7. The largest increases in shrub with corresponding decreases in bare occurred in the higher biomass graminoid and shrub classes (i.e. 1–3, 5–6). By contrast, more sparsely vegetated classes typically located at higher elevations demonstrated limited changes in the shrub and herbaceous fractions. Note that these alpine communities are strongly controlled by topographic factors that limit soil development, moisture, and nutrient supply (Walker 2000).

An independent accuracy assessment of the fractional changes is challenging owing to the lack of repeat vegetation observations, a frequent problem for Arctic change studies. One means of corroborating the trends and increasing confidence in the results is to compare them with observations from published studies documenting different types of surface changes within the study domain. Here we present two available examples.

Vegetation resource inventories were conducted within the study area in 1985–1986 on Herschel Island and in 1988–1989 on Ivvavik's coastal plain (Kennedy 2008; C. Kennedy, personal communication, 2010). These biophysical inventories involved comprehensive surveys of vegetation, soil, and surficial geology at several hundred sites. A study was later conducted to investigate if significant vegetation changes were occurring on these sites. Subsequent field observations found that, within 12–15 years, cover of the native grass species (polargrass, *Arctagrostis latifolia*) had significantly

https://doi.org/10.1017/S0032247411000477 Published online by Cambridge University Press

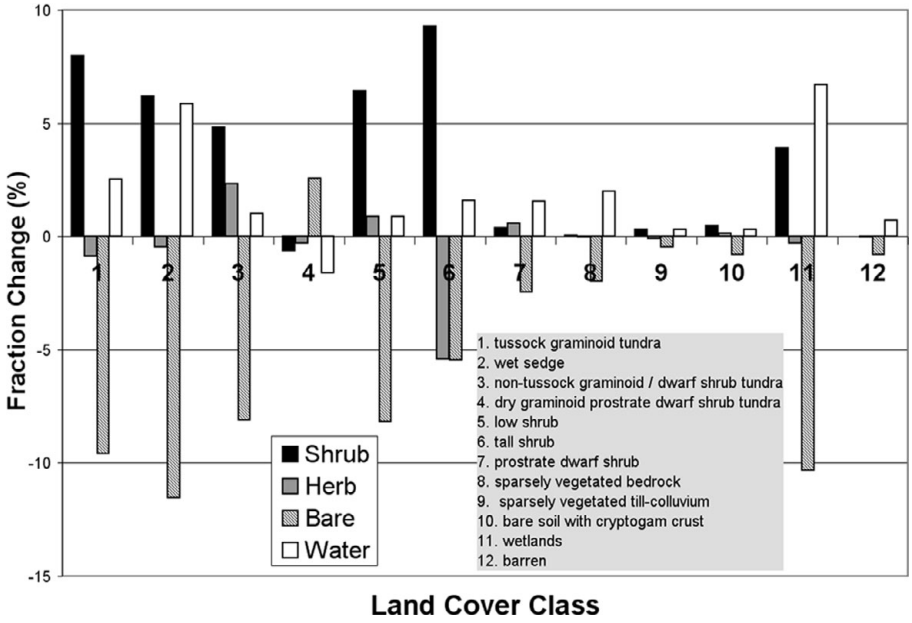

Fig. 7. Average change in fractional land cover between 1985 and 2009 over the study area by land cover type.

increased on upland sites. There was also an increase in low shrub and decrease in lichen and bare ground. Polargrass and Arctic lupin (*L. arcticus*) were also found to have increased in cottongrass tussock sites on Herschel Island but not on the coastal plain.

Overall, the results from the Landsat trend and fractional change analysis are consistent with these observations. We found that Kennedy's study area, shown using the dashed line in Fig. 5, coincides with the strongest positive trends in TC greenness (Figs. 5, 8). On Herschel Island, estimated herbaceous land cover increased on average by 9% (Fig. 8), shrubs increased by 10%, and bare ground cover decreased by 21%. The trends are also directionally compatible with long term sample plot measurements taken about 300 km to the west of the study area in the foothills of the Brooks Range in Alaska.

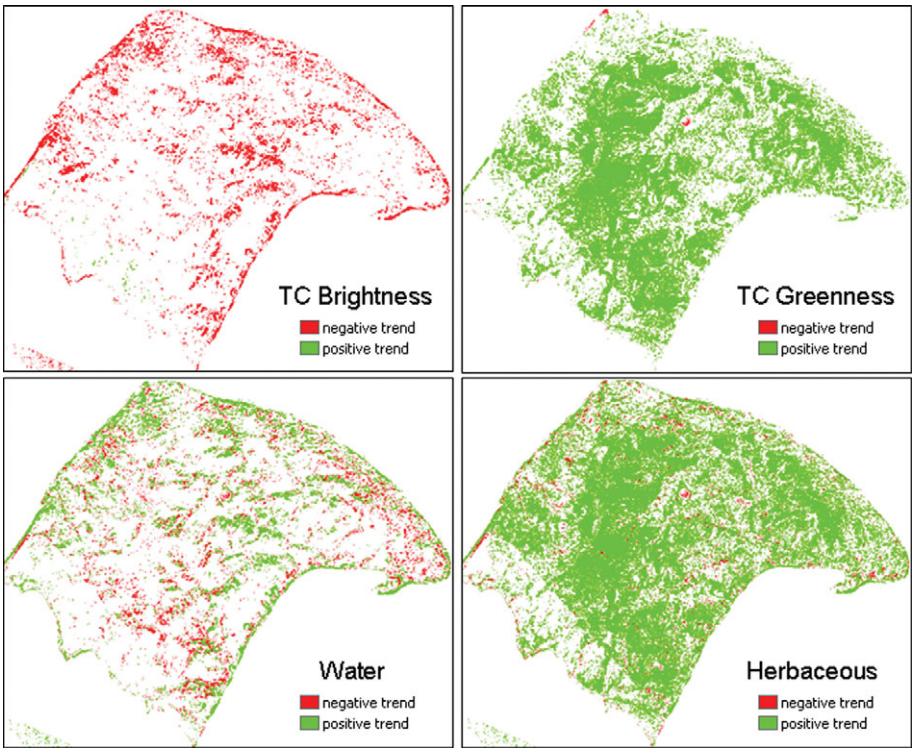

Fig. 8. 1985–2009 change in Tasseled Cap Brightness and Greenness indices, and in water and herbaceous land cover fractions over Herschel Island.

https://doi.org/10.1017/S0032247411000477 Published online by Cambridge University Press

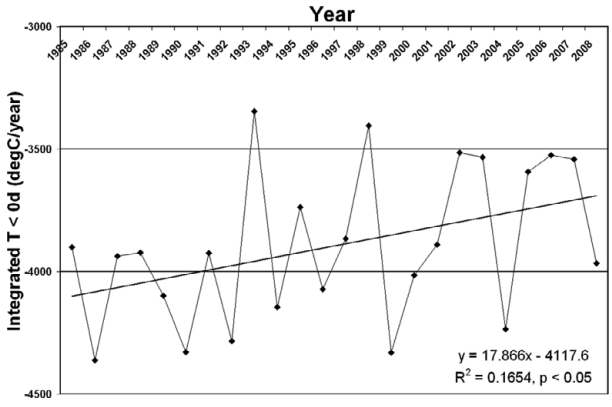

Fig. 9. 1985–2008 annual integrated temperature less than zero degrees Celsius for the study area based on the National Centers for Environmental Prediction (NCEP) North American Regional Reanalysis (NARR) dataset.

In this moist tussock tundra site, shrub and graminoid cover increased by 60–80% from 1989 to 2008 (Gould and others 2009).

Discussion

Recent increases in Arctic shrub abundance are best explained by longer and warmer growing seasons promoting plant growth (Goetz and others 2005; Jia and others 2009) and increasing nutrient mineralisation and availability (Chapin and others 1995). However, in the study region, available climate reanalysis and weather station data suggest a trend towards milder winters (Fig. 9) but little change in summer air temperatures. A mechanism that could permit increased shrub growth in the absence of warmer growing seasons is described in Sturm and others (2005). They propose a positive feedback effect in which shrub growth leads to locally deeper snow, which promotes higher winter soil temperatures, greater microbial activity, and more plant-available nitrogen. High levels of soil nitrogen then favour shrub growth the following summer. Note that increased winter soil temperatures and nutrient mineralisation might also be expected from milder winters in northern Yukon, independent of any shrub feedback effect (for example Hill and Henry 2010).

A second source of corroboration is a study of coastal erosion and thaw slumping on Herschel Island caused by melting of ice rich permafrost. Lantuit and Pollard (2008) calculated mean coastal retreat rates of 0.61 m/yr and 0.45m/yr for the periods 1952–1970 and 1970–2000 using orthorectified airphotos and Ikonos imagery. Maximum shoreline retreat during 1970–2000 was 54 m, equivalent to about two Landsat pixels. Increased retrogressive thaw slump activity was also observed between 1952 and 2000 on the southeast facing shorelines. We found that the TC brightness trend was particularly sensitive to coastal erosion on Herschel, while this change was also evident as an increasing water fraction (Fig. 8). Here, the strong declines resulted from a vegetated land surface being replaced by water or wet soil, both of which are dark surfaces.

The regression tree models used to generate the above results were trained using TC trend values corresponding to the acquisition date of the high resolution training image. The major argument in favour of a trend based change method is that it allows long term directional change to be more reliably discerned from inter-scene/annual sources of variation, such as those related to illumination, atmosphere, surface moisture, and phenology. To evaluate the potential magnitude and impact of this shorter term variation, additional regression trees were trained using the Landsat TM scene from 24 July 2005 and then applied to both this scene and the ETM+ scene from 26 July 2006. Comparing the predicted fractions for common clear sky pixels, average 2006–2005 differences were −2.7% for bare, +0.2% for herbaceous, +2.2% for shrub, and +0.2% for water. Considering that these scenes are only one year apart and fall within the peak 10 day NDVI period (21–30 July), this may represent the lower end of ephemeral variability expected from a conventional two date change approach. Such an approach could therefore lead to incorrect conclusions regarding directional vegetation change.

There are potential limitations of the regression tree change detection approach that should be considered. First, a necessary assumption in applying the trees to estimate fractional change is that the accuracy of the models when applied through time will be comparable to their spatial accuracy (Table 3). At present, the required field measurements are not available to make a quantitative assessment of the models' temporal predictions. A further assumption is that the trees trained over a portion of the study domain are representative and similarly accurate when applied over the larger area. However, studies have demonstrated that accuracy of fractional cover estimates drops with geographical distance from the training site (Fernandes and others 2004; Olthof and Fraser 2007). Clearly, it is important to select a training area that represents the full range of vegetation conditions found throughout the study area. Finally, the high resolution land cover classification used to quantify fractional composition of 30 m Landsat training pixels was based on a hard classification of shrub, herbaceous, bare, and water. Even at 1–4 m resolution, these classes are normally mixed in the Arctic and a label must be assigned to the dominant class. Further investigation is warranted to determine if model accuracy improves if vegetation composition from small field quadrats is used to create a high-resolution fractional classification for training (Fig. 2).

The major advantage of a Landsat-based trend detection method over coarse resolution (1–8 km) change approaches is the ability to resolve vegetation change with greater spatial resolution. As an example, the most striking change observed over the study area was increasing greenness and foliar vegetation growth along the coastline and on Herschel Island. Yet, a 1985–2006 trend

https://doi.org/10.1017/S0032247411000477 Published online by Cambridge University Press

analysis using 1 km NOAA-AVHRR data (Pouliot and others 2009) did not detect this area as having significant changes in NDVI. This is not surprising considering that increasing TC greenness was observed only over 7.6% of our study area.

Summary and conclusions

This paper described a change detection method suitable for long term analysis of northern vegetation at local to regional scales. It employs a temporally dense stack of Landsat TM/ETM+ imagery from 1985 to present to reveal trends in reflectance indices associated with vegetation and other physical changes to the landscape. Regression trees are then used to convert the reflectance trends into a more meaningful metric of change in bare, shrub, herbaceous, and water fractional land cover. The method was found to be sensitive to growth of vascular vegetation and coastline erosion that were documented by independent sources. It is argued that a trend based Landsat change method is preferable to a standard two scene analysis to separate longer term directional change in vegetation from potentially high inter-variability in tundra vegetation conditions.

The approach is now being applied over four national parks in northern Canada (Ivvavik, Wapusk, Torngat Mountains, and Sirmilik). Preliminary results, to be reported in a follow up paper, reveal a range of corroborated changes, including wildfire, damage to vegetation by geese, glacier retreat, and general increases in vascular vegetation in three of the parks. It is anticipated that Parks Canada Agency will employ the satellite based change products and methods for deriving measures of ecological integrity for State of the Park reporting required for each park every five years. A protocol manual and tutorial dataset is being prepared to allow the methods to be used by Parks Canada staff.

Acknowledgements

This work was partially funded by the Canadian Space Agency Government Related Initiatives Programme (GRIP). We are grateful for the support and helpful advice from many Parks Canada Agency employees including, but not limited to, Donald McLennan, Paul Zorn, Jean Poitevin, Rajeev Sharma, and Justin Quirouette.

References

Bhatt, U.S., D.A. Walker, M.K. Raynolds, J.C. Comiso, H.E. Epstein, G. Jia, R. Gens, J.E. Pinzon, C.J. Tucker, C.E. Tweedie, and P.J. Webber. 2010. Circumpolar Arctic tundra vegetation change is linked to sea-ice decline. *Earth Interactions* 14: 1–20.

Boelman, N.T., M. Stieglitz, K.L. Griffin, and G.R. Shaver. 2005. Inter-annual variability of NDVI in response to long-term warming and fertilization in wet sedge and tussock tundra. *Oecologia* 143: 588–597.

Buus-Hinkler, J., B.U. Hansen, M.P. Tamstorf, and S.B. Pedersen. 2006. Snow-vegetation relations in a High Arctic ecosystem: Inter-annual variability inferred from new monitoring and modeling concepts. *Remote Sensing of Environment* 105: 237–247.

Chander, G., B.L. Markham, and D.L. Helder. 2009. Summary of current radiometric calibration coefficients for Landsat MSS, TM, ETM+, and EO-1 ALI sensors. *Remote Sensing of Environment* 113: 893–903.

Chapin, F. S. III, G.R. Shaver, A.E. Giblin, K.J. Nadelhoffer, and J.A. Laundre. 1995. Responses of arctic tundra to experimental and observed changes in climate. *Ecology* 76: 694–711.

Cohen, W.B., T. Spies, R.J. Alig, D.R. Oetter, T.K. Maiersperger, and M. Fiorella. 2002. Characterizing 23 years (1972–95) of stand replacement disturbance in western Oregon forests with Landsat imagery. *Ecosystems* 5: 122–137.

Crist, E.P., and R.C. Cicone. 1984. A physically-based transformation of thematic mapper data—The TM tasseled cap. *IEEE Transactions on Geoscience and Remote Sensing* GE-22: 256–263.

Dowdeswell, E.K., J.A. Dowdeswell, and F. Cawkwell. 2007. On the glaciers of Bylot Island, Nunavut, Arctic Canada. *Arctic, Antarctic, and Alpine Research* 39: 402–411.

Epstein, H.E., M.P. Calef, M.D. Walker, F.S. Chapin III, and A.M. Starfield. 2004. Detecting changes in arctic tundra plant communities in response to warming over decadal time scales. *Global Change Biology* 10: 1325–1334.

Fernandes, R., R. Fraser, R. Latifovic, J. Cihlar, J. Beaubien, and Y. Du. 2004. Approaches to fractional land cover and continuous field mapping: a comparative assessment over the BOREAS study region. *Remote Sensing of Environment* 89: 234–251.

Fraser, R.H., I. Olthof, and D. Pouliot. 2009. Monitoring land cover change and ecological integrity in Canada's national parks. *Remote Sensing of Environment* 113: 1397–1409.

Goetz, S., A. Bunn, G. Fiske, and R. Houghton. 2005. Satellite-observed photosynthetic trends across North America associated with climate and fire disturbance. *Proceedings of the National Academy of Sciences of the United States of America* 102: 13521–13525.

Goodwin, N.R., N.C. Coops, M.A. Wulder, and S. Gillanders. 2008. Estimation of insect infestation dynamics using a temporal sequence of Landsat data. *Remote Sensing of Environment* 112: 3680–3689.

Gould, W., J.A. Mecado Diaz, and J.K. Zimmerman. 2009. Twenty year record of vegetation change from long-term plots in Alaskan tundra. Estes Park, CO: LTER (LTER all scientists meeting 'Integrating science and society in a world of constant change, 14–16 September 2009). URL: http://asm.lternet.edu/2009/posters/twenty-year-record-vegetation-change-long-term-plots-alaskan-tundra

Hill, G.B., and G.H.R. Henry. 2010. Responses of a High Arctic wet sedge tundra to climate warming since 1980. *Global Change Biology* doi:10.1111/j.1365–2486.2010.02244.x.

Huang, C., B. Wylie, L. Yang, C. Homer, and G. Zylstra. 2002. Derivation of a tasselled cap transformation based on Landsat 7 at-satellite reflectance. *International Journal of Remote Sensing* 23: 1741–1748.

Huang, C., S.N. Goward, J.G. Masek, N. Thomas, Z. Zhu, and J.E. Vogelmann. 2010. An automated approach for reconstructing recent forest disturbance history using dense Landsat time series stacks. *Remote Sensing of Environment* 114, 183–198.

Hudson, J.M.G., and G.H.R. Henry. 2009. Increased plant biomass in a High Arctic heath community from 1981 to 2008. *Ecology* 90: 2657–2663.

Irish, R.R., J.L. Barker, S.N. Coward, and T. Arvldson. 2006. Characterization of the Landsat-7 ETM+ automated cloud-cover assessment (ACCA) algorithm. *Photogrammetric Engineering and Remote Sensing* 72: 1179–1188.

Jia, G.J., H.E. Epstein, and D.A. Walker. 2009. Vegetation greening in the Canadian Arctic related to warming and sea ice decline. *Journal of Environmental Monitoring* 11: 2231–2238.

Kendall, M.G., and A.S. Stuart. 1967. *Advanced theory of statistics*. Vol. 2. London: Charles Griffin and Company.

Kennedy, C. 2008. Vegetation change on Herschel Island and the Ivvavik coastal plain. Pg 110–114 In: Keeping track. Whitehorse: Environment Yukon (2007 Yukon north slope conference. Environmental monitoring and reporting in wildlife management. Summary report). URL: http://www.wmacns.ca/pdfs/224_2007_NSC-SummaryReport.pdf

Kennedy, R.E., W.B. Cohen, and T.A. Schroeder. 2007. Trajectory-based change detection for automated characterization of forest disturbance dynamics. *Remote Sensing of Environment* 110: 370–386.

Kennedy, R.E., Z. Yang, and W.B. Cohen. 2010. Detecting trends in forest disturbance and recovery using yearly Landsat time series: 1. LandTrendr — temporal segmentation algorithms. *Remote Sensing of Environment* 114: 2897–2910.

Labrecque, S., D. Lacelle, C. Duguay, B. Lauriol, and J. Hawkings. 2009. Contemporary (1951–2001) evolution of lakes in the Old Crow Basin, Northern Yukon, Canada: remote sensing, numerical modelling, and stable isotope analysis. *Arctic* 62: 225–238.

Lantuit, H., and Pollard W.H. 2008. Fifty years of coastal erosion and retrogressive thaw slump activity on Herschel Island, southern Beaufort Sea, Yukon Territory, Canada. *Geomorphology* 95: 84–102.

Latifovic, R., Trishchenko A.P., Chen J., Park W.B., Kholpenkov K.V., Fernandes R., Pouliot D., Ungureanu C., Luo Y., Wang S., Davidson A., and Cihlar J. 2005. Generating historical AVHRR 1 km baseline satellite data records over Canada suitable for climate change studies. *Canadian Journal of Remote Sensing* 31: 324–346.

Mars, J.C., and D.W. Houseknecht. 2007. Quantitative remote sensing study indicates doubling of coastal erosion rate in past 50 yr along a segment of the Arctic coast of Alaska. *Geology* 35: 583–586.

Olthof, I., and R.H. Fraser. 2007. Mapping northern land cover fractions using Landsat ETM+. *Remote Sensing of Environment* 107: 496–509.

Olthof, I., D. Pouliot, R. Latifovic, and W. Chen. 2008. Recent (1986–2006) vegetation-specific NDVI trends in Northern Canada from satellite data. *Arctic* 61: 381–394.

Olthof, I., R. Latifovic, and D. Pouliot. 2009. Development of a circa 2000 land cover map of northern Canada at 30 m resolution from Landsat. *Canadian Journal of Remote Sensing* 35: 152–165.

Parks Canada Agency. 2009. Ivvavik National Park of Canada: natural environment. URL: http://www.pc.gc.ca/pn-np/yt/ivvavik/natcul/natcul1.aspx

Pouliot, D., R. Latifovic, and I. Olthof. 2008. Detection and evaluation of NDVI trends in Canada from 1985–2006. *International Journal of Remote Sensing* 30: 149–168.

Riedel, S.M., H.E. Epstein, and D.A. Walker. 2005. Biotic controls over spectral reflectance of arctic tundra vegetation. *International Journal of Remote Sensing* 26: 2391–2405.

Riordan, B., D. Verbyla, and A.D. McGuire. 2006. Shrinking ponds in subarctic Alaska based on 1950–2002 remotely sensed images. *Journal of Geophysical Research* 111: G04002

Röder, A., T. Udelhoven, J. Hill, G. del Barrio, and G. Tsiourlis. 2008. Trend analysis of Landsat-TM and -ETM +imagery to monitor grazing impact in a rangeland ecosystem in Northern Greece. *Remote Sensing of Environment* 112: 2863–2875.

Selkowitz, D.J.. 2010. A comparison of multi-spectral, multi-angular, and multi-temporal remote sensing datasets for fractional shrub canopy mapping in Arctic Alaska. *Remote Sensing of Environment* 114: 1338–1352.

Silapaswan, C.S., D.L. Verbyla, and A.D. McGuire. 2001. Land cover change on the Seward Peninsula: the use of remote sensing to evaluate the potential influences of climate warming on historical vegetation dynamics. *Canadian Journal of Remote Sensing* 27: 542–554.

Stow, D.A., B.H. Burns, and A.S. Hope. 1993. Spectral, spatial and temporal characteristics of Arctic tundra reflectance. *International Journal of Remote Sensing* 14: 2445–2462.

Stow, D.A., A. Hope, D. Mcguire, D. Verbyla, J. Gamon, F. Huemmrich, S. Houston, C. Racine, M. Sturm, K. Tape, L. Hinzman, K. Yoshikawa, C. Tweedie, B. Noyle, C. Silapswan, D. Douglas, B. Griffith, G. Jia, H. Epstein, D. Walker, S. Daeschner, A. Petersen, L. Zhou, and R. Myneni. 2004. Remote sensing of vegetation and land-cover change in Arctic tundra ecosystems. *Remote Sensing of Environment* 89: 281–308.

Sturm, M., C. Racine, and K. Tape. 2001. Increasing shrub abundance in the Arctic. *Nature* 411: 546–547.

Tape, K., S. Matthew, and C. Racine. 2006. The evidence for shrub expansion in Northern Alaska and the Pan-Arctic. *Global Change Biology* 12: 686–702.

Vogelmann, J.E., B. Tolk, and Z. Zhu. 2009. Monitoring forest changes in the southwestern United States using multitemporal Landsat data. *Remote Sensing of Environment* 113: 1739–1748.

Walker, D.A. 2000. Hierarchical subdivision of Arctic tundra based on vegetation response to climate, parent material and topography. *Global Change Biology* 6: 19–34.

Walker, M.D., C.H. Wahren, R.D. Hollister, G.H.R. Henry, L.E. Ahlquist, J.M. Alatalo, M.S. Bret-Harte, M.P. Calef, T.V. Callaghan, A.B. Carroll, H.E. Epstein, I.S. Jónsdóttir, J.A. Klein, B. Magnússon, U. Molau, S.F. Oberbauer, S.P. Rewa, C.H. Robinson, G.R. Shaver, K.N. Suding, C.C. Thompson, A. Tolvanen, A., Ø Totland, P.L. Turner, C.E. Tweedie, P.J. Webber, and P.A. Wookey. 2006. Plant community responses to experimental warming across the tundra biome. *Proceedings of the National Academy of Sciences* 103: 1342–1346.

Xu, M., P. Watanachaturaporn, P.K. Varshney, and M.K. Arora. 2005. Decision tree regression for soft classification of remote sensing data. *Remote Sensing of Environment* 97: 322–336.

https://doi.org/10.1017/S0032247411000477 Published online by Cambridge University Press